Article

JOURNAL OF COMPOSITE MATERIALS

Journal of Composite Materials
2014, Vol. 48(13) 1623–1636

DOI: 10.1177/0021998313488807
jcm.sagepub.com

SAGE

The mechanical behavior of composite corrugated core coated with elastomer for morphing skins

Iman Dayyani[1,2], Saeed Ziaei-Rad[1] and Michael I Friswell[2]

Abstract

Coated composite corrugated panels have wide applications in engineering, especially in morphing skins where extreme anisotropic stiffness properties are required. The optimal design of these structures requires high-fidelity models of the panels that would be incorporated into multi-disciplinary system models. Therefore, numerical and experimental investigations are required that retain the dependence on the nonlinear static and dynamic behavior of these structures. Considering the nonlinear effects due to the material properties and mechanism of deformation, the mechanical behavior of composite corrugated laminates with elastomeric coatings is studied in this paper by means of numerical and experimental investigations. The importance of this work is that it provides detailed experimental and numerical models of the panel that can be used for further static and dynamic homogenization and optimization studies. In this regard, an investigation of the manufacturing method and an evaluation of the mechanical characteristics of the materials are presented. Then the tensile, hysteresis and three-point bending tests of the coated corrugated panels are analyzed and the mechanical behavior of the panel is simulated. The comparison studies demonstrate the accuracy of the finite element model to predict the mechanical behavior of the coated corrugated panels. Finally, two concepts to deal with the non-smooth surface of the panel during bending for the morphing skin application are proposed.

Keywords

Glass fibers, elastomer, mechanical testing, finite element simulation, morphing skin

Introduction

Sandwich structures have been used extensively for applications where the weight of the member is important, such as packaging, civil, naval, automotive and aerospace industries, due to their low mass-to-stiffness ratio and high-impact absorption capacity.[1–5] Some instances of their applications in daily life are cardboard sandwich cores used for packaging, metal corrugated roofs, ship hulls, automotive chassis and bumpers, fuselages and morphing wings. In nature, where mechanical performance has to be optimized, sandwich structures are used, for example the human skull which is made up of two layers of dense compact bone separated by a ''core'' of lower density material.

Composite corrugated panels, as a subdivision of sandwich structures, have exceedingly anisotropic behavior. They are stiff and flexible along and transverse to the corrugation direction, respectively. Composite corrugated panels have been proposed as a candidate for application in morphing wings. This is because the wing structure must be stiff to withstand the bending due to aerodynamic forces and flexible to deform to match the most efficient form in the flight regime. Another advantage of using sandwich structures (made of metals or composites) with corrugated cores is that they have high fatigue resistance. Moreover, composite corrugated panels decrease the number of parts used in a wing structure, which increases the speed of assembly and reduces the manufacturing costs.[6]

[1]Department of Mechanical Engineering, Isfahan University of Technology, Isfahan, Iran
[2]College of Engineering, Swansea University, Swansea, UK

Corresponding author:
Saeed Ziaei-Rad, Department of Mechanical Engineering, Isfahan University of Technology, Isfahan 84156-83111, Iran.
Email: szrad@cc.iut.ac.ir

Numerous investigations have been carried out on the bending stiffness of corrugated board. Luo et al.[7] reported an analytical study on the bending stiffness of corrugated board. They considered different shapes of the corrugated medium including sinusoidal, arc-and-tangent and elliptical representations. Gilchrist et al.[8] studied the mechanical behavior of corrugated board using finite element analysis and included both geometric and material nonlinearities in their model. They examined in-plane and transverse loadings of corrugated board configurations and their results from the finite element analysis correlated reasonably well with the experimental measurements. Daxner et al.[9] conducted an optimization study of a specific kind of corrugated board with the aim of weight-reduction. Their optimization scheme resulted in a set of parameters describing a new design of corrugated core which reduced the specific weight by more than 18% and maintained the buckling strength of the original design. Kazemahvazi and Zenkert[10,11] tested and developed monolithic and hierarchical corrugated composite cores with better strength properties. They demonstrated that the hierarchical structures exhibit a range of different failure modes when the material and geometrical properties of the structure are altered. Leekitwattana et al.[12] proposed an interesting concept of bi-directional corrugated structures. Their study focused on the derivation of the transverse shear stiffness of a sandwich beam structure using analytical methods. They validated the transverse shear stiffness with a three-dimensional finite element model and evaluated the effect of geometrical parameters of the corrugated structure.

The development of smart materials motivated designers to reconsider the concept of morphing wings which may provide superior aircraft performance. Morphing wings are an important application of coated corrugated panels and in many cases the design of the skins has been recognized as a major issue. The highly anisotropic behavior of composite corrugated panels is very effective in morphing wing applications; the panels are stiff along the corrugations to withstand the aerodynamic loads and flexible transverse to the corrugations to allow deformation. Figure 1 shows a schematic application of the coated corrugated core as a skin of the Fish-BAC morphing trailing edge device.[13]

Yokozeki et al.[14] proposed carbon composite corrugated board as a candidate material for morphing wings. They evaluated the in-plane stiffness and strength of corrugated board through tensile and bending tests in the longitudinal and transverse directions. In addition, they developed a simple analytical model for the initial stiffness of the corrugated core.

Thill et al.[15–17] carried out tensile and flexural experimental testing of trapezoidal corrugated laminates both longitudinally and in transverse to the corrugation directions. They investigated the effect of various materials and parameters, such as number of plies and corrugation pitch, on the overall mechanical properties of the corrugated structure and realized that the transverse tensile elastic modulus is dependent on the laminate thickness squared and total corrugated profile unit cell length. They explained the obtained results via experimental, analytical and numerical analysis methods and concentrated particularly on the local failure mechanisms and the material behavior around the corner region of the corrugated unit cell. The three-stage mechanical behavior of the composite corrugated core in the tensile test was found in their work which is

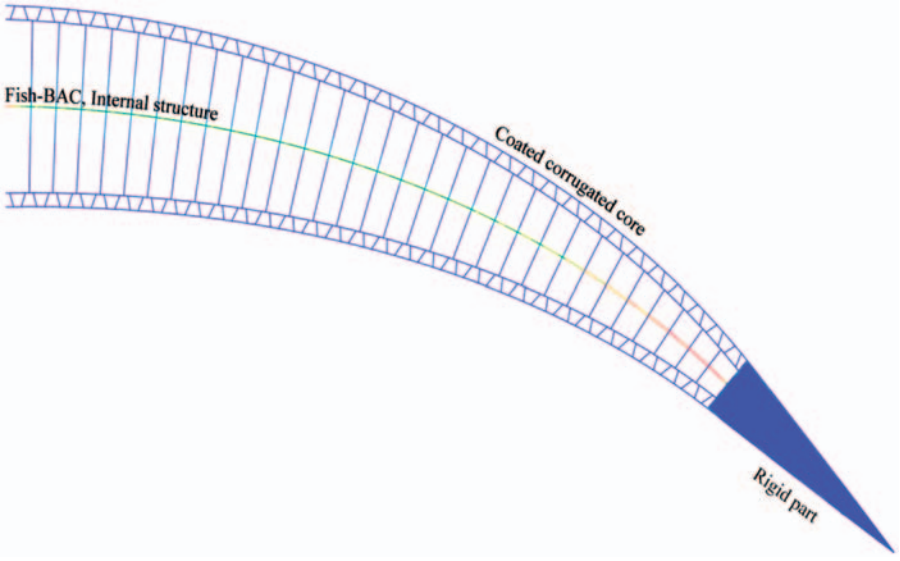

Figure 1. Schematic application of the coated corrugated core on the fish-BAC morphing trailing edge concept.

unlikely to occur in glass or carbon fiber reinforced corrugated laminates. Moreover, they carried out wind tunnel testing of the morphing skin panel concept and identified its limitations. A segmented skin was suggested to improve the performance of the panel. Their study concluded that morphing skin panel concept exploiting corrugated sandwich structures offers a potential solution for local morphing wing skins for low speed and small air vehicles.

Xia et al.[18] studied the analytical homogenization model of corrugated cores to reduce the size of the finite element models. They considered both the in-plane and the out-of-plane local deformations of the corrugated sheet and demonstrated the efficient performance of the homogenization for morphing wing applications.

Dayyani et al.[19] used experimental, numerical and analytical methods to study the tensile and flexural characteristics of a composite corrugated core made of glass fibers. They assigned plastic behavior to the whole structure in order to model the energy dissipation due to delamination. In contrast to the material of the literature, they showed that the three-stage mechanical behavior of composite corrugated cores is not confined to aramid corrugated laminates and can be observed in other types of laminates.

Although significant efforts have been devoted to research into adaptive structures and morphing aircraft, examples of practical solutions are still very few. For the first time, the tensile, hysteresis and flexural performance of coated composite corrugated cores is studied by means of numerical and experimental investigations.

Finally, two concepts to deal with the non-smooth surface of the panel during bending, which is the main aerodynamic disadvantage of such structures in morphing applications, are proposed in this paper.

Problem definition

Coated core fabrication

The composite corrugated cores were manufactured using a trapezoidal machined aluminium mould. Prepreg laminates of glass fiber plain woven cloth were hand-laid by use of a heat gun to ease the forming process. Using an inverted trapezoidal aluminium mould and weights to compress the stacked prepreg laminates, the desired thickness was obtained and then the vacuum bagging process was performed. More details of the manufacturing process as well as schematics of the trapezoidal mould and the prepreg glass fiber laminates are presented in the authors' previous work.[19] The corrugated laminates were cured for an hour at 160°C under vacuum pressure.

After curing, both the upper and lower surfaces of the corrugated core were coated with elastomeric skins by use of fiberglass silicone adhesive, to improve the aerodynamic surfaces of the panel for the morphing skin application. In terms of the study of mechanics of fluids, the elastomer coating would improve the aerodynamic surfaces of the panel which would result in a higher lift to drag ratio over the trailing edge of the wing. In terms of mechanics of solids and structural analysis, the elastomeric skin functions like a combination of spring and damper which is parallel with the corrugated core and resists the deformation and damps the vibration of the whole structure. The skins were polymers which generally have viscoelastic behavior, low Young's modulus, large yield strain and high damping. This polymeric material is widely used in applications where low stiffness and high elastic strains are required. Considering the anisotropic behavior of the elastomeric skins and the application of the panel to morphing wings, the corrugated core was coated in the more compliant direction (Figure 4(b)). This way of coating would give a more flexible structure along the chord-wise direction that requires less actuation force for the global deformation of the trailing edge and a stiffer structure along the span-wise direction, which means the elastomer coating has more stiffness to resist the bending due to the aerodynamics forces.

Coated core geometry

The length of the coated composite corrugated core investigated in this paper was 300 mm; however, the widths of the tensile and bending test specimens were 25 mm and 100 mm, respectively. Figure 2(a) shows the

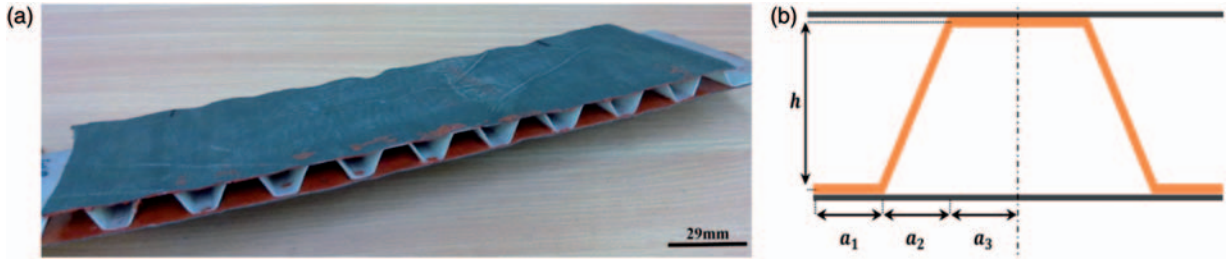

Figure 2. The coated composite corrugated core and the geometry of a unit cell.

constructed coated composite corrugated core. The thicknesses of the corrugated core and elastomer skins were 1.00 mm and 0.80 mm, respectively. Other dimensions of the corrugated core are given in Figure 2(b), and the corresponding parameters are listed in Figure 2(b) and are tabulated in Table 1.

Coated core material characterization

The corrugated core was made of three-plies of woven glass fibers with epoxy resin. Some of the benefits of fiber glass are their relatively low price, high tensile strength, high chemical resistance and good insulating properties.[20] In terms of mechanical properties, composites with epoxy resin can replace metal parts such as steel in aerospace and industrial applications and they often perform better than the metal components. High adhesion, good resistance to fatigue and moisture penetration are some of the exclusive mechanical properties of epoxy resin.[21] The orientations of the plies were 0°, 90° with respect to the corrugation direction.

Table 1. Dimensions of the corrugated core unit cell.

Dimensions	Values
a_1	3.75 mm
a_2	5.5 mm
a_3	5.3 mm
h	9.5 mm

To evaluate the mechanical properties of the composite material, a total of five flat specimens were manufactured with the procedure described in section "*Coated core fabrication*," but using flat aluminium plates and spacers. The specimens were end-tabbed using 0/ 90 glass-epoxy laminates and Araldite adhesive for the tensile testing. The length, width and thickness of the tabbed sections were 50 mm, 15 mm and 5 mm, respectively. It is noticeable that the gauge length, width and thickness of the un-tabbed regions of the specimens were 150 mm, 15 mm and 1.1 mm, respectively. Moreover, uniaxial tensile tests in standard environmental conditions were carried out on samples to measure the material properties of the composite corrugated core. Figure 3 illustrates the experimental stress–strain curves for five flat specimens in tension.

Figure 3 shows that the stress–strain curves of glass fiber laminates are almost linear. The maximum stress

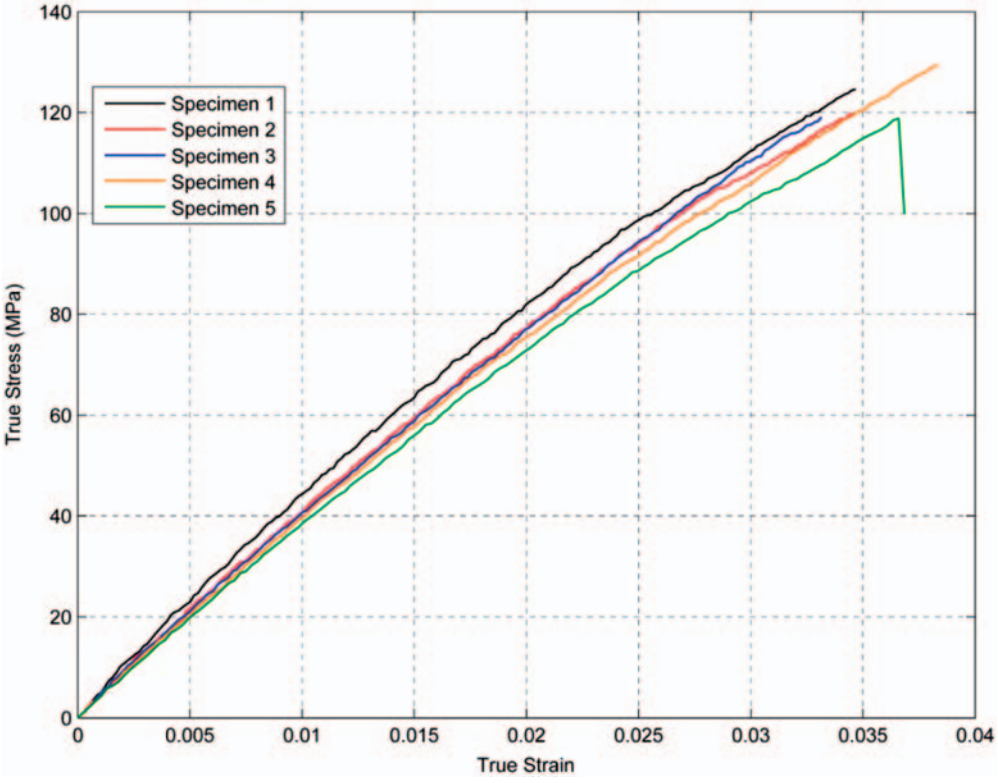

Figure 3. Stress-strain curves for uniaxial tests on flat specimens.

reached is 120.6 MPa, where the sample experienced a brittle failure at a strain of 0.03508. The ratio of failure strain to stress also demonstrates the high tensile strength of composites made of glass fiber. Poisson's ratios are calculated from the ratio of transverse strain to axial strain measured by extensometers with appropriate accuracy. Moreover, the shear moduli in the longitudinal and transverse directions for the composite laminates are provided from the manufacturer. The material properties of the investigated prepreg are given in Table 2.

The upper and lower skins of the sandwich panel are both made of elastomers that are composed of long chains of entangled molecules, which are mostly made of carbon atoms. The behavior of elastomers are very complex; on the macroscopic scale, they usually behave initially as elastic isotropic but become anisotropic at finite strain as the molecule chains tend to realign to the loading direction.[22] Some of the characteristics of this class of polymers are their low density of cross-links[23] as well as their ability to undergo large elastic deformations without long-lasting changes in shape. In other words, the elastomers show hyper-elastic behavior. Abrasion resistance, resilience, flame retardance and UV light resistance are other characteristics of the elastomers.[24]

Table 2. Material properties of the composite corrugated core.

Properties	Corrugated core
E_1	4.5 GPa
E_2	4.5 GPa
ν_{12}	0.225
G_{12}	3 GPa
G_{13}	3 GPa
G_{23}	3 GPa

The elastomer coatings used in this paper were made of synthetic rubber, namely polyurethane (PU). The PU threads were knitted by a circular interlock weft method. In this type of knitting, one continuous thread runs crosswise in the fabric making all of the loops in one course. Consequently, the woven fabric has a smooth surface on both sides, as well as fairly good shape retention and possesses good wearing qualities.[25] The skin was made from a chloroprene polymer designed for the use in high-strength application and flexible adhesives,[26,27] two laminates of elastomeric woven fabrics were pressed, adhered together and then cured at room temperature.

The mechanical properties of the elastomer were evaluated using a total of six strips of elastomer sheets that were cut in the longitudinal and transverse directions. The length, width and thickness of the elastomeric strips were 150 mm, 25 mm and 0.85 mm, respectively. Using a Zwick testing machine with a load cell of 1 kN, the specimens were tested in tension. ASTM D412[28] was used as a basis for the tensile standard testing and the tests were carried out under displacement control at a rate of 10 mm/min for elastomeric specimens. Figure 4(a) shows the elastomeric coating specimen in the tensile testing machine. Figure 4(b) illustrates the stress–strain curves of six elastomer specimens in the longitudinal and transverse directions, respectively.

Figure 4(b) demonstrates one of the distinctive characteristics of elastomers, namely their large elastic deformation capacity. The elastomeric specimens stretched 1.5 and 3.3 times over their original lengths in the longitudinal and transverse directions, respectively. Furthermore, the elastomer presents a softening

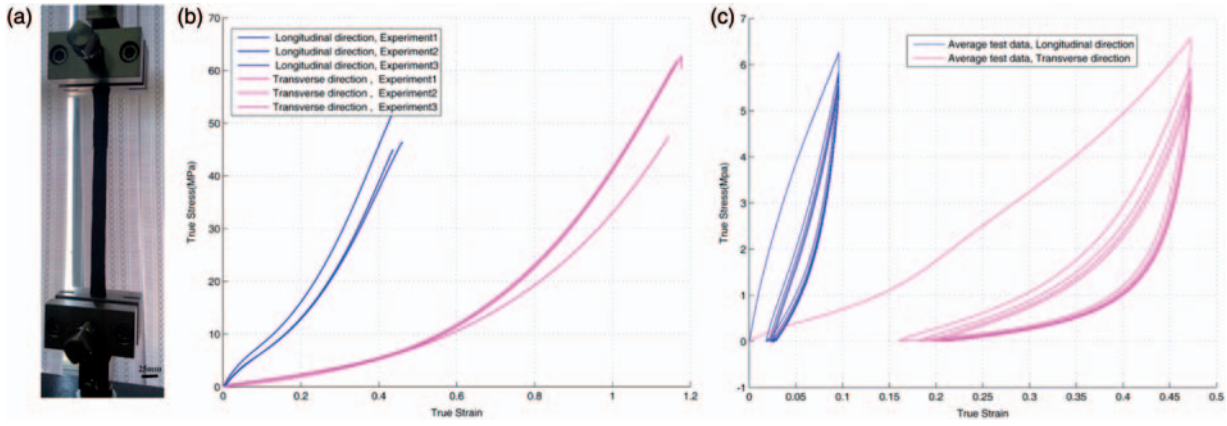

Figure 4. The tensile test of the elastomer specimens in the longitudinal and transverse directions. (a) Test set-up, (b) stress-strain curves and (c) average hysteresis curves.

Table 3. The Young's modulus of the elastomer in the longitudinal and transverse directions.

True strain	Initial stretch	Medium stretch	Final stretch
Young modulus in longitudinal direction	88.60 MPa	57.18 MPa	162.22 MPa
Young modulus in transverse direction	14.00 MPa	10.25 MPa	108.00 MPa

behavior in medium stretching stage in both longitudinal and transverse directions as described in Table 3.

However, as portrayed in Figure 4(b), the ratios of the final tensile stresses and final tensile strains of the elastomer in the transverse-to-longitudinal directions are 1.33 and 2.7, respectively; this is another reason to align the elastomer on the corrugated composite core as mentioned in section "*Coated core fabrication*." In addition, the Poisson's ratios are calculated by the ratio of transverse strains to axial strains measured by the extensometers.

The material damping, also known as internal friction or hysteresis, is associated with energy dissipation in the volume of a macro-continuous medium. This phenomenon arises when a homogeneous volume of material is subjected to cyclic loading at constant amplitude. The damping mechanism is usually related to the material microstructure. Generally, elastomers can fail due to either thermal fatigue or mechanical fatigue. The failure is caused by factors such as load frequency, stress level, temperature and the geometry of the component.

For elastomers, their fatigue life is affected by parameters such as the size and distribution of the initial defects and stress concentrations within the sample geometry. The fatigue performance is also affected by processing, molecular distribution, as well as the degree of cross-linking in the microstructure, and environmental influences such as test temperature and exposure to aggressive chemicals.[29]

The independent investigation of the fatigue behavior of elastomeric coatings is important for morphing skin applications, because the elastomeric coatings are subjected to air flow that may generate cyclic stresses in the elastomeric skins. To evaluate the cyclic loading behavior of elastomers, a total of six strips were cut in the longitudinal and transverse directions. The length, width and thickness of the elastomeric strips as well as displacement rate and environmental conditions were identical to the static testing. Figure 4(c) illustrates the average stress–strain hysteresis curves of the elastomer specimens in the longitudinal and transverse directions.

Figure 4(c) shows that when the elastomeric test specimen is subjected to tension from its virgin state, unloaded and then reloaded, the stress required for reloading is less than the initial loading for stretches up to the maximum stretch achieved during the initial loading. This stress-softening phenomenon is known as the Mullins effect, which is frequently observed in filled rubber elastomers as a result of damage associated with straining at the microscopic level.[30] In other words, by loading the material, the damage occurs by severing the bonds between the filler particles and the rubber molecular chains. Different chain links break at different deformation levels, thereby leading to continuous damage with macroscopic deformation. An equivalent explanation is that the energy required to cause the damage is not recoverable. Furthermore, the loading-unloading cycles for any given strain level do not occur along a single curve, and there is some hysteresis. There is also some permanent deformation upon removal of the applied load. The graphs also represent evidence of progressive damage with repeated cycling at any given maximum strain. The response appears to stabilize after a number of cycles. Based on these observations, the area of the hysteresis loops decreases over the initial cycles and reaches equilibrium after a few cycles. The dissipated energy in one cycle of dynamic testing in the longitudinal direction is 4.82 times smaller than that in the transverse direction.

Experiments on coated composite corrugated core

Tensile test of coated composite corrugated core

Using a Zwick testing machine with a load cell of 1 kN, six specimens of the coated composite corrugated core were subjected to tensile test in the direction transverse to their corrugations. ASTM D3039 [31] is used as a basis for the tensile standard testing. The tests were performed under displacement control at a rate of 2 mm/min for coated corrugated core specimens. Figure 5(a) illustrates the investigated composite corrugated core with elastomeric coatings in the tensile test.

During the test on the uncoated structure, delamination was detected by the abrupt sounds mainly due to the deboning of layers. This phenomenon influenced the behavior of the corrugated core in tension. Optical microscopy was undertaken on the delaminated regions of the unit cells of the corrugated core. The samples were then investigated using stereomicroscopy. Figure 6 shows microscopic images of delaminations in the specimen during the tensile testing. However, in contrast to the uncoated corrugated core, the elastomeric coatings

Figure 5. Tensile test of the composite corrugated core with elastomeric coatings.

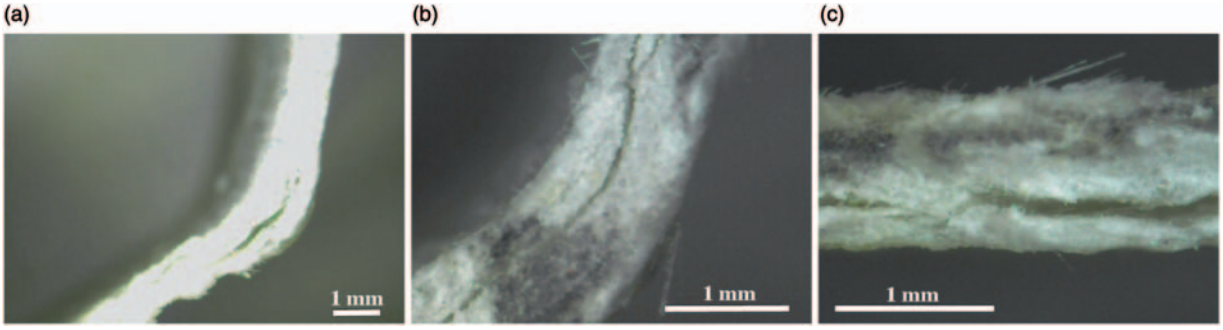

Figure 6. Microscopic images of delamination in the trapezoidal corrugated specimen region during tensile testing.

damped and reduced the effect of delamination on the whole sandwich panel. The rubber sheets function as parallel springs to the corrugated core and increase the total stiffness of the sandwich panel. Since the elastomers have good damping characteristics, they dissipate the sudden impacts imposed on the corrugated core due to delamination. Figure 7 shows a comparison of the average data corresponding to the corrugated core with and without elastomeric coatings.

Figure 7 indicates the mechanical behavior of the coated corrugated core in two main phases: A and B. Phase A occurs before the failure of the corrugated core and is divided into three distinct stages. The first stage, which was due to the small deformation of the horizontal and inclined members of the corrugated core, has a linear trend. Considering the low tensile stiffness of the corrugated core in the initial stages, the effect of elastomer is evident in this stage. The skin functioned like a stiff spring parallel with the corrugated core and resisted the deformation of the whole structure.

In the second stage, the unit cell corners of the corrugated core rotated like a joint due to delamination and required less force in comparison with the force needed for the deformation in the first stage. Therefore, the resistance of elastomer to tension is more marked and consequently the difference between

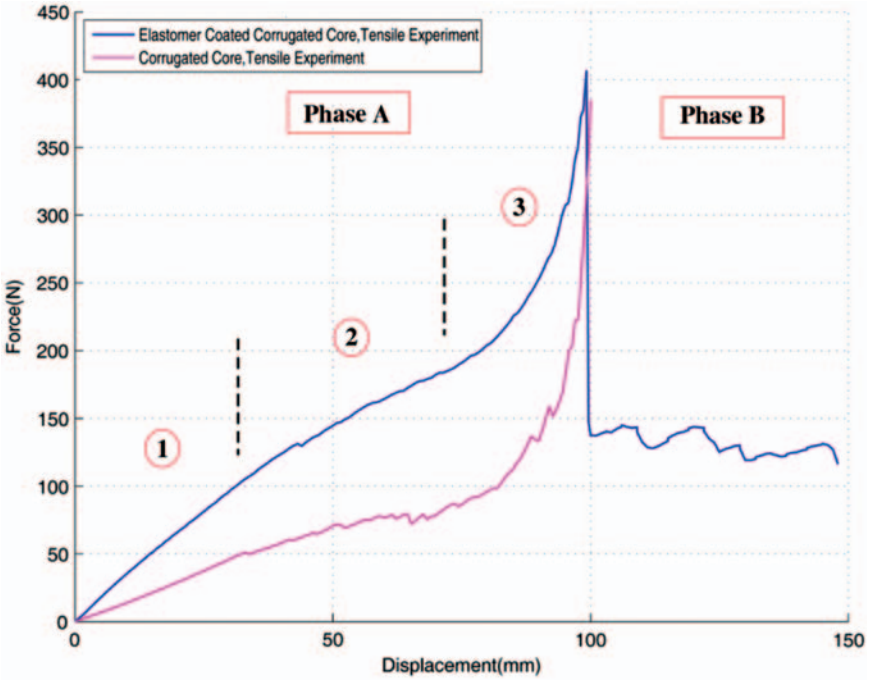

Figure 7. A comparison of the mechanical properties of the corrugated core with and without elastomeric coatings.

the graphs corresponding to the coated and uncoated cores increases.

In the third stage, the corners of the corrugated core were rotated and consequently the structure had an almost flattened shape. The distance between the curves of coated and uncoated corrugated cores decreased with increasing displacement. This phenomenon arises because the Young's modulus of the elastomer was negligible in comparison to the Young's modulus of glass fiber laminates when both the corrugated core and elastomer coating were fully stretched.

Moreover, as shown in Figure 7, when the elongation exceeds 100 mm, the corrugated core fails. Since the elastomer coatings have larger elongation capacity and due to the strong adhesion between the corrugated laminates of glass fibers and elastomeric coatings, only the coatings were exposed to tension. The mechanical behavior of the structure in this configuration is depicted as phase (B) in Figure 7.

Hysteresis test on coated composite corrugated cores

Structural components subjected to cyclic stress can yield due to fatigue, causing them to fail at stress levels much lower than with static mechanical loading. Therefore, the cyclic loading behavior of composite corrugated cores with and without elastomeric coating for morphing skin applications, where the source of cyclic stresses may be the aerodynamic flow over the skin or the actuation force deforming the trailing edge, is important.

It is difficult to observe hysteresis in engineering materials by using conventional methods, but it can be demonstrated using high-precision measurements. Using a Zwick testing machine with a load cell of 1 kN, a total of four specimens of coated and uncoated composite corrugated core were tested dynamically over 10 cycles, transverse to their corrugations. The length, width and thickness of both coated and uncoated specimens were the same as the static testing. However, these tests were carried out under displacement control at a rate of 50 mm/min. Both coated and uncoated composite corrugated cores were tested, each at a different maximum displacement. The maximum displacements were selected before and after the elastic limit as illustrated in Figure 8. It must be mentioned that by elastic limit, the authors mean the limit in which the delamination cracks initiate and start dissipating the strain energy of the structure. In other words, any kind of deviation from the perfect linear elasticity irrespective of its nature is referred to as inelasticity.[32] (More details are presented in section "*Tensile test simulation*.") For two sets of the investigated specimens, the maximum displacements were selected as 30 mm and 60 mm, respectively. Figure 8 shows the comparison of 10 hysteresis loops of each set.

Figure 8(a) highlights the fact that although both specimens were tested before the elastic limit, the uncoated corrugated core, in contrast to the coated corrugated core, possesses an ideal linear force-displacement characteristic. Considering the special mechanical properties of fiber glass and elastomer

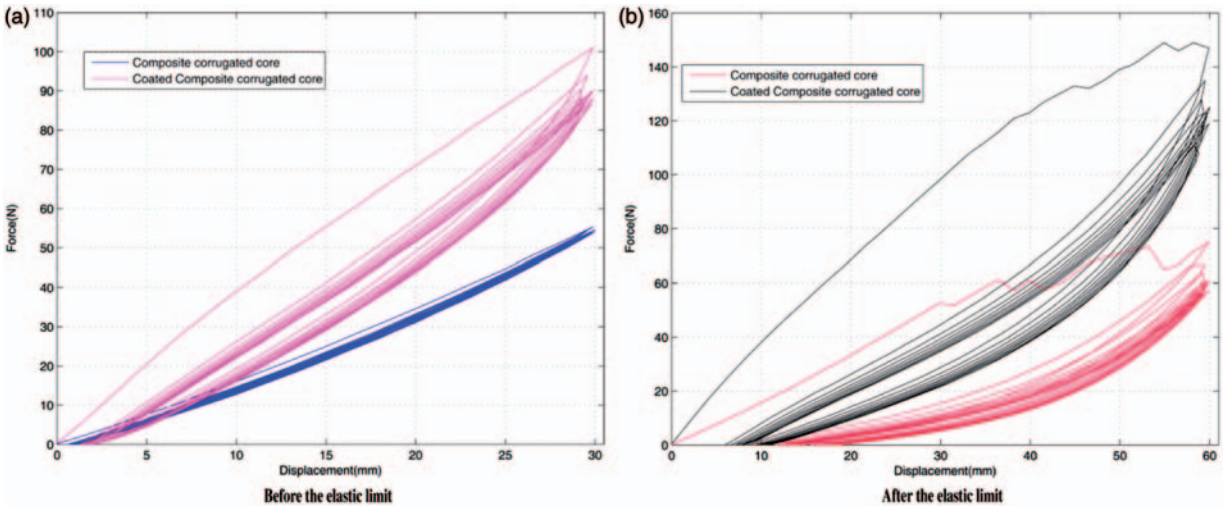

Figure 8. Hysteresis loops for each set of specimens at different maximum displacements.

discussed in section "*Coated core material characterization*," such a behavior can be explained. Since the behavior of the fiber glass is almost perfectly elastic, the amount of energy dissipated in the material upon one loading-unloading cycle is negligible. On the other hand, due to Mullins effect, observed frequently in filled rubber elastomers, the microscopic damage results in considerable energy dissipation.

Figure 8(b) illustrates the hysteresis behavior of both coated and uncoated composite corrugated core beyond the elastic limit. As mentioned before, the sharp peaks in the loading path indicate delamination, which is the main factor in dissipating the strain energy of the composite corrugated core and consequently resulting in a shift in the hysteresis loops. Considering the delamination effect and Figure 8(b), it is apparent that the amount of energy dissipation in the specimens after the static limit upon one loading-unloading cycle is more than those specimens before the static limit.

Three-point bending test of the coated composite corrugated core

Using a Zwick testing machine with a load cell of 1 kN, six specimens of the coated composite corrugated core were tested with a three-point bending test. ASTM C393[33] was used as the bending standard test for sandwich structures. The span and diameter of the support rollers were 193 mm and 5 mm, respectively. The tests were under displacement control at a rate of 5 mm/min for the coated corrugated core specimens. Figure 9 shows the testing machine and the coated composite corrugated core during the three-point bending test.

Figures 9 and 11(b) show that the mechanical behavior of the sandwich panel can be classified into three phases: the first phase in which the supports are in contact with the elastomer reinforced by the corrugated

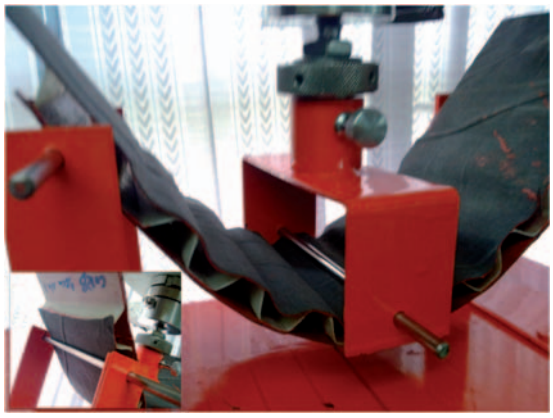

Figure 9. Testing machine and the coated corrugated core during the three-point bending test.

core, the second phase in which the support is only in contact with the elastomer coating and the third phase in which the trend is similar to the first one. The elastomer sheet functioned as a membrane and therefore did not withstand any bending moment, since the lower elastomer was in tension; phase two had a minor effect on the mechanical behavior of the sandwich panel in the three-point bending test. Moreover, the upper elastomer coating was buckled due to the compressive forces. This non-smooth surface of the panel during bending is a main aerodynamic disadvantage of the structure for morphing skin applications and is discussed more in section "*Novel coated composite corrugated core concept*."

Finite element analysis

Tensile test simulation

First, in order to model the true behavior of the elastomeric coated corrugated core, the core was subjected to a

Table 4. Plastic material properties estimated from experimental data.

Plastic strain	Plastic stress (MPa)
0.0000	37.35
0.0052	58.19
0.0103	64.53
0.0150	85.00
0.0300	95.00
0.0500	105.00
0.0800	140.00
0.1800	240.00

tensile test. During the test, the composite laminates of the corrugated core were subjected to bending moments which caused high inter-laminar stresses. These stresses resulted in delamination and crack propagation in the corrugated core. In this mode of failure, the strain energy of the composite corrugated core was dissipated.

Many of the mechanisms concerned with plastic deformation are not yet sufficiently identified. Therefore, the processes involved in the inelastic behavior are generally termed plastic deformation damping. Modeling the dissipation of energy, a plastic material model for the corrugated core was specified. In this paper, an elastic-plastic model is specified for the corrugated core. The details of the failure mechanism and corresponding modeling technique in tensile loading are presented in the authors' previous work.[19] The orthotropic linear elastic material properties of the model are presented in Table 2. The plastic stress–strain values were tuned from Figure 7 to obtain a better correlation between experimental data and predicted values. The tuned plastic stress–strain values are listed in Table 4.

Figure 5(a) shows that the boundary conditions for the tensile experiment were modeled so that all degree of freedom except the translational displacement in the longitudinal direction of the panel were fixed. To discretize the corrugated composite core, four-node doubly curved quadrilateral shell elements using reduced integration and hourglass control were used.

Second, the elastomer coatings were modeled as a hyperelastic material defined by the uniaxial test data illustrated in Figure 4(b). The prediction of material behavior under different deformation modes was compared to the experimental data and fitted to an Ogden strain energy potential of order 3. The Ogden strain energy potential corresponding to an incompressible material is expressed in terms of the principal stretches. Based on reference [34], the following formulation is used:

$$U = \sum_{i=1}^{3} \frac{\mu_i}{\alpha_i}(\lambda_1^{\alpha_i} + \lambda_2^{\alpha_i} + \lambda_3^{\alpha_i} - 3) \quad (1)$$

Table 5. The coefficients corresponding to the Ogden strain energy potential of order 3.

$\mu_1 = -3.63601012$	$\mu_2 = 0.005112819957$	$\mu_3 = 10.2501705$
$\alpha_1 = 1.66716812$	$\alpha_2 = 12.320745$	$\alpha_3 = -11.1400669$

where $\lambda_1, \lambda_2, \lambda_3$ are the principal stretches satisfying the constraint

$$\lambda_1\lambda_2\lambda_3 = 1 \quad (2)$$

Table 5 represents the coefficients corresponding to this strain energy potential. Only the compliant direction of the elastomer coating is modeled using the nonlinear formulation since the stiffer direction is perpendicular to the tension. Moreover, since the ratio of elastomer Young's modulus to glass fiber Young's modulus is very small, the elastomer coatings are neglected in the areas overlapped with the composite corrugated core. This assumption is valid because these two materials are well adhered together and have the same displacement. Thus, the strain energy of the elastomer is very small compared to the strain energy of the glass fiber in the overlapped areas.

The upper and lower elastomeric coatings were modeled with both four-node quadrilateral membrane and shell elements with reduced integration and hourglass control and there was no appreciable difference between the results. This was due to the fact that in both the tensile and three-point bending tests, the upper and lower elastomeric coatings were subjected to only axial forces. In other words, the bending stiffness of the shell elements corresponding to the elastomeric coatings may be neglected. Therefore, to make the model simpler and to reduce the computational cost and time (especially in the three-point bending test in which there was contact between the support and the coatings), shell elements are used. The large deflection option incorporating geometric nonlinearities into the formulation was considered.

Figure 10 illustrates the simulation of coated composite corrugated core in tension, as well as a comparison of force-displacement behavior in tension obtained from the experiment and ABAQUS simulation.

Figure 10(b) shows that a close correlation is apparent in first two stages of phase A (as discussed in section "*Tensile test of coated composite corrugated core*"). However, the graph corresponding to the simulation deviates slightly from the experiment curve in stage three. This small deviation in stage three may be because the delamination is not modeled, which dissipates strain energy. In other words, since the effect of delamination has been modeled by a typical plastic behavior, the corners of the corrugated core rotate

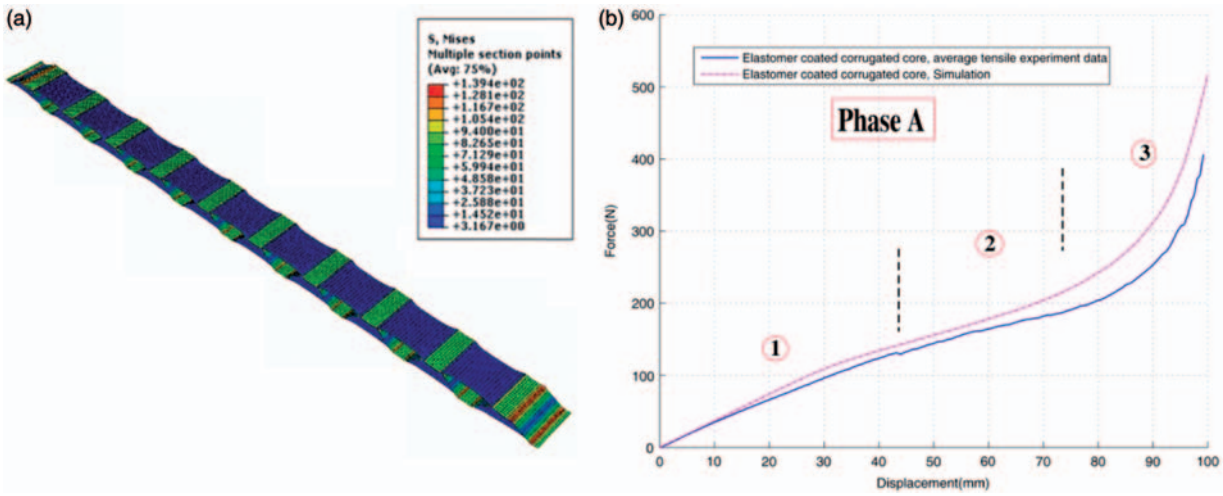

Figure 10. Simulation of the coated composite corrugated core in tension and comparison of force-displacement behavior from experiment and simulation.

more easily than the real deformation mechanism. As a result, the corrugated core experiences flattening in simulation sooner than the real structure. Thus, for a constant displacement in stage three, the force predicted by the simulation is higher than that recorded in the experiment.

Three-point bending test simulation

A morphing skin must be flexible enough to minimize the actuation force required to change the camber profile and stiff enough to resist the aerodynamic forces encountered during flight. In addition, the skin must remain elastic throughout its use, so there would be no change in the surface of the wing, which could produce unwanted air flow characteristics. For the designed composite corrugated core as a candidate of morphing skin, the bending deformation is a concern for its significant influence on the aerodynamic performance of the morphing aircraft. Therefore, one of the goals of this paper is to investigate the mechanical behavior of the coated composite corrugated core in bending. In this section, a finite element simulation of the three-point bending test is presented.

Having two axes of symmetry, a quarter of the coated corrugated composite core was modeled in ABAQUS. The support was modeled as a rigid rod having no degrees of freedom. Node to surface and friction-less contact formulations were used for the interaction between the corrugated core and the supports. Figure 11(a) illustrates the simulation of the coated corrugated core in the three-point bending test.

Again, geometric nonlinearities were considered in the formulation. By using four-node quadrilateral shell elements with reduced integration and hourglass control, the corrugated composite core and coatings were discretized. The element size in the contact region was 1 mm, which was two to three times smaller than the element size in the other regions. A mesh convergence study was performed to confirm the mesh independency of the solution. Figure 11(b) illustrates a comparison between the force-displacement behavior at the center of the coated corrugated core in three-point bending from the experiment and simulation results.

In Figure 11(b), the mechanical behavior of the coated corrugated core in bending includes three different phases. In the first and third phases, the supports are in contact with the elastomer reinforced with the corrugated core which means that the coated corrugated core is exposed to pure three-point bending. In contrast, in the second phase the support is in contact with the elastomer only. Since the elastomer acts as a membrane and withstands only in-plane tensile forces, the force reduces slightly.

Novel coated composite corrugated core concept

As mentioned in section "*Three-point bending test simulation*," the non-smooth surface of the coated composite corrugated core is a disadvantage for the aerodynamics in a morphing skin application. However, this fault can be modified in two ways. First, the elastomer coatings should be pre-stretched and then adhered to the corrugated core. In this method the coatings are still in tension even if their position is compressed during bending. Figure 7 shows that separation between the elastomer coatings and the composite corrugated core occurs for forces over 400 N. This means that the adhesive is resistant to separation for the tensile displacements required in order to stretch the buckled coatings.

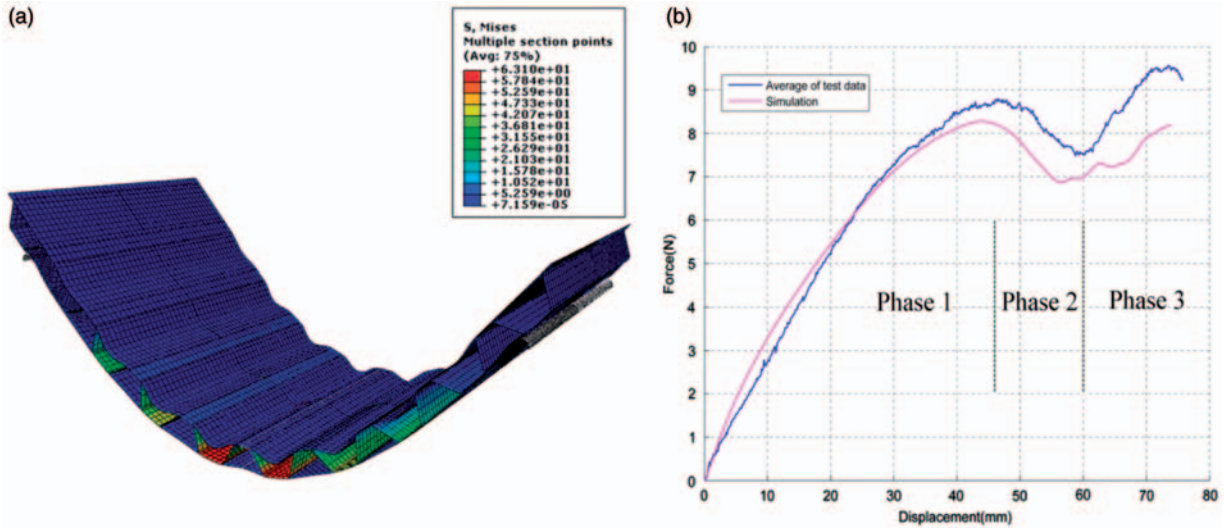

Figure 11. Simulation of the coated corrugated core in the three-point bending test and comparison of the force-displacement behavior from experiment and simulation.

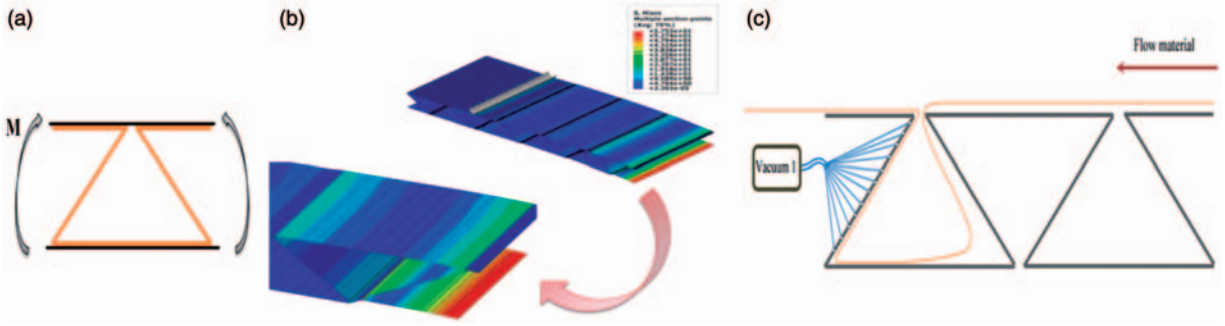

Figure 12 Schematic of the unit cell, a quarter of the coated triangular corrugated core in pure bending, and the corresponding manufacturing concept.

Second, by changing the geometry of a unit cell of the corrugated core into a triangular shape, the gap where the elastomer coating buckles would reduce. Consequently, the ratio of area corresponding to the elastomer coatings reinforced with corrugated core to the area of the elastomer coatings which is not reinforced, would increase. The gap between the corners of two adjacent unit cells of the corrugated core would also close as the bending increases. Figure 12(a) shows a schematic of the unit cell of a triangular composite corrugated core coated with elastomer in pure bending. When the symmetric loading is applied to the unit cell of Figure 12(a), the gap would close completely. However, since the loading in each unit cell of the sandwich panel is not symmetric, the sharp corners of the unit cell of the corrugated core do not exactly meet and one corner slides over the other and the perfect gap closure between adjacent corners of the structure would not be accomplished, as illustrated in Figure 12(b).

The sketch of triangular corrugate core must be modified so that the deformed geometry of panel has smooth surfaces in the desired bending position. This requires extra analytical and numerical investigations to predict the position of the members of the deformed corrugated core coated with elastomer. Optimizing the length of the members and angle of corners is necessary to obtain the smooth surfaces in the desired position of the panel.

Novel coated composite corrugated core manufacturing concept

The triangular composite corrugated core may be manufactured using a triangular machined aluminium mould. However, the triangular mould could be made of other material such as plaster. The advantage and disadvantage of a plaster mould is reduced cost of production and life-time of the mould, respectively. A number of holes must be made in the surfaces of

all members of the mould in order to connect the vacuum set to the mould.

First, laminates of glass fiber woven cloth must be laid in the first unit cell of the mould. Then the first surface of the unit cell is vacuumed through the embedded holes. A heat gun might be used to ease forming of the prepregs into the corners of the mould. After that the vacuum corresponding to the second surface would be activated while the first vacuum is active. This procedure would continue for the third surface. Figure 12(c) shows a schematic of the proposed manufacturing process of the triangular coated composite corrugated core.

A rod with triangular section area may be fit in the first unit cell of the mould. This would compress the stacked prepreg laminates and therefore the desired thickness would be obtained. Next, the laminate can be cured under vacuum pressure or pressure from the rods. The corrugated core would then be coated by elastomer.

Conclusions

Using numerical and experimental investigations, tensile, hysteresis and flexural characteristics of a composite corrugated core with elastomer coatings has been investigated in this paper. The composite corrugated cores were fabricated using a trapezoidal machined aluminium mould. Then, both upper and lower surfaces of the corrugated core were covered by elastomer coatings.

Evaluating the mechanical properties of the material, a series of simple tension tests were performed on the standard samples of composite laminates as well as elastomeric strips. The linear stress–strain curves of glass fiber laminates demonstrated the high tensile strength of composites made of glass fiber. The elastomeric specimens stretched 1.5 and 3.3 times over its original length in longitudinal and transverse directions, respectively, which illustrates one of the distinctive characteristics of elastomers, i.e. their large elastic deformation capacity. Stress softening phenomenon was also investigated experimentally in the longitudinal and transverse directions of the elastomer. Moreover, cyclic loading behavior of the elastomers was also studied experimentally in the longitudinal and transverse directions. It was shown that the dissipated energy in one cycle of dynamic testing in the longitudinal direction is 4.82 times smaller than that in the transverse direction.

Next, the coated composite corrugated cores were subjected to tensile, cyclic loading and three-point bending tests. The tensile behavior of the coated corrugated core was classified into two main phases: phase A and phase B, which are before and after the failure of the corrugated core. In addition, phase A was subdivided into three distinguished stages. The effect of the elastomeric coatings on the overall behavior of the structure was significant only in the first two stages. Furthermore, due to the perfect elongation capacity of the elastomer coatings and strong adhesion between the corrugated laminates of glass fiber and the elastomeric coatings, after failure of the corrugated core, only the coatings were exposed to tension in phase B.

Two sets of specimens were subjected to cyclic loading before and after the elastic limit and the energy dissipation was compared. The mechanical behavior of the coated corrugated core in bending has been categorized into three phases: the first phase in which the supports were in contact with the elastomer reinforced with corrugated core, the second phase in which the support was only in contact with the elastomer coating and the third phase in which the trend was similar to the first phase.

Numerical solutions were proposed to simulate the recorded force-displacement response of the panels in tensile loading and bending. A good degree of correlation was observed which showed the suitability of the finite element model to predict the mechanical behavior of coated corrugated laminate panels.

The non-smooth surface of corrugated panels during bending is one of the main aerodynamic limitations of the structure for morphing skin applications. Two concepts were proposed to deal with this drawback: the composite corrugated core covered with pre-stretched coating and a triangular corrugated core with elastomer coating.

Conflict of Interest

None declared.

Funding

This research received no specific grant from any funding agency in the public, commercial, or not-for-profit sectors.

References

1. Wang D. Impact behavior and energy absorption of paper honeycomb sandwich panels. *Int J Impact Eng* 2005; 36: 110–114.
2. Tipping S and Stojadinovic B. Innovative corrugated steel shear walls for multi-story residential buildings. In: *14th World Conference on Earthquake Engineering*, Beijing, China, 12–17 October 2008, Paper number: #05-06-0105.
3. Ning H, Janowski GM, Vaidya UK, et al. Thermoplastic sandwich structure design and manufacturing for the body panel of mass transit vehicle. *Compos Struct* 2007; 80: 82–91.
4. McGowan DM and Ambur DR. Damage-tolerance characteristics of composite fuselage sandwich structure with thick face sheets. National aeronautics and space administration, Langley Research Center, Hampton, Virginia, 1997, 23681-0001, NASA Technical Memorandum, 110303.

5. Heimbs S, Middendorf P, Hampf C, et al. Aircraft sandwich structures with folded core under impact load. In: *8th international conference on sandwich structures*, ICSS 8 A, (ed AJM Ferreira), Porto, Portugal, 6–8 May, 2008, pp. 369–380.
6. Degussa Röhm GmbH & Co. KG, Fatigue behaviour of sandwich foam core materials –comparison of different core materials, Pg-Tp-Sa, Kirschenallee, D-64293 Darmstadt, Germany.
7. Luo S, Suhling JC, Considine JM, et al. The bending stiffness of corrugated board. *Mech Cellul Mater ASME* 1992; 36: 15–26.
8. Gilchrist AC, Suhling JC and Urbanik TJ. Nonlinear finite element modeling of corrugated board. *Mech Cellul Mater SME* 1999; 231: 101–106.
9. Daxner T, Flatscher T and Rammerstorfer FG. Optimum design of corrugated board under buckling constraints. In: *7th world congress on structural and multidisciplinary optimization*, COEX Seoul, Korea, 2007, pp. 349–358.
10. Kazemahvazi S and Zenkert D. Corrugated all-composite sandwich structures. Part 1: Modeling. *Compos Sci Technol* 2009; 69: 913–919.
11. Kazemahvazi S and Zenkert D. Corrugated all-composite sandwich structures. Part 2: Failure mechanisms and experimental programme. *Compos Sci Technol* 2009; 69: 920–925.
12. Leekitwattana M, Boyd SW and Shenoi RA. Evaluation of the transverse shear stiffness of a steel bi-directional corrugated-strip-core sandwich beam. *J Const Steel Res* 2011; 67: 248–254.
13. Woods BKS and Friswell MI. Preliminary investigation of a fishbone active camber concept. In: *Proceedings of the ASME 2012 conference on smart materials, adaptive structures and intelligent systems*, September 19–21, Paper no. 8058. Georgia, United States: ASME.
14. Yokozeki T, Takeda S, Ogasawara T, et al. Mechanical properties of corrugated composites for candidate materials of flexible wing structures. *Compos A* 2006; 37: 1578–1586.
15. Thill C, Etches JA, Bond IP, et al. Corrugated composite structures for aircraft morphing skin applications. In: *18th international conference of adaptive structures and technologies*, Ottawa, Ontario, Canada, 2007.
16. Thill C, Etches JA, Bond IP, et al. Investigation of trapezoidal corrugated aramid/epoxy laminates under large tensile displacements transverse to the corrugation direction. *Compos A* 2010; 41: 168–176.
17. Thill C, Etches JA, Bond IP, et al. Composite corrugated structures for morphing wing skin applications. *Smart Mater Struct* 2010; 19(124009).
18. Xia Y, Friswell MI and Saavedra Flores EI. Equivalent models of corrugated panels. *Int J Solid Struct* 2012; 49: 1453–1462.
19. Dayyani I, Ziaei-Rad S and Salehi H. Numerical and experimental investigations on mechanical behavior of composite corrugated core. *J Appl Compos Mater* 2012; 19: 705–721.
20. Forbes Aird. *Fiberglass & composite materials*. 1st ed. United States: Penguin, 1996.
21. Clayton A May. *Epoxy resins: Chemistry and technology*. 2nd ed. New York: CRC Press, 1988.
22. Harper CA. *Handbook of plastics, elastomers & composites*. 4th ed. New York: McGraw-Hill, 2002.
23. Callister WDJ. *Materials science and engineering: An introduction*. 7th ed. Wiley, 2006.
24. Bhowmick AK and Stephens H. *Handbook of elastomers*. 2nd ed. CRC Press, 2000.
25. Wake WC and Wootton DB. *Textile reinforcement of elastomers*. Applied Science Publishers, 1982.
26. Ebnesajjad S. Handbook of adhesives and surface preparation: Technology, applications and manufacturing, William Andrew 2010.
27. Damico DJ. *Advances in adhesives, adhesion science, and testing*, No. 1463. ASTM International, 2005.
28. Standard test methods for vulcanized rubber and thermoplastic elastomers-tension, [ASTM D 412-98a]. American National Standards Institute. West Conshohocken, Pa; Annual book of ASTM Standards, 2002; 09.01: 43–55.
29. Hainsworth SV. An environmental scanning electron microsopy investigation of fatigue crack initiation and propagation in elastomers. *Polymer Test* 2007; 26: 60–70.
30. Ogden RW and Roxburgh DG. A pseudo-elastic model for the Mullins effect in filled rubber. *Proc Royal Soc London, Series A* 1999; 455: 2861–2877.
31. Standard test method for tensile properties of polymer matrix composite materials. D 3039/D 3039M-08. test Conshohocken, PA: ASTM International, 2008.
32. Frunza Gh. Elemente de Plasticitate şi Mecanica Ruperii, EDP, Bucuresti, 2005; pp. 256–270.
33. Standard Test Method for flexural properties of sandwich constructions, C393-00. test Conshohocken, PA: ASTM International, 2000.
34. Ogden RW, Saccomandi G and Sgura I. Fitting hyperelastic models to experimental data. *Computational Mech* 2004; 34: 484–502.
35. ABAQUS 6.11-2, SIMULIA, 2011.